



ELSEVIER

Available online at www.sciencedirect.com

ScienceDirect

journal homepage: www.intl.elsevierhealth.com/journals/dema

Ceria-incorporated MTA for accelerating odontoblastic differentiation via ROS downregulation

Soo-Kyung Jun^{a,b}, Ji-Young Yoon^{b,c}, Chinmaya Mahapatra^{b,c},
Jeong Hui Park^{b,d}, Hae-Won Kim^{a,b,c,d}, Hyung-Ryong Kim^b,
Jung-Hwan Lee^{a,b,c,d,*}, Hae-Hyung Lee^{a,b,d,**}

^a Department of Biomaterials Science, School of Dentistry, Dankook University, Cheonan 330-714, South Korea

^b Institute of Tissue Regeneration Engineering (ITREN), Dankook University, Cheonan 330-714, South Korea

^c Department of Nanobiomedical Science & BK21 PLUS NBM Global Research Center for Regenerative Medicine Research Center, Dankook University, Cheonan 330-714, South Korea

^d UCL Eastman-Korea Dental Medicine Innovation Centre, Dankook University, Cheonan 31116, Republic of Korea

ARTICLE INFO

Article history:

Received 24 March 2019

Received in revised form

30 May 2019

Accepted 30 May 2019

Keywords:

Ceria nanoparticle

ROS downregulation

Mineral trioxide aggregate

Dental pulp stem cells

ABSTRACT

Objective. Odontoblast differentiation from dental pulp stem cells (DPSCs) is involved in a cascade of key biological events for maintaining pulp-dentin homeostasis, repair and regeneration. A pulp regeneration biomaterial (mineral trioxide aggregate (MTA)) increased intracellular reactive oxygen species (ROS) levels during differentiation, ameliorating the differentiating of DPSCs into odontoblasts. Here, ceria nanoparticles (CNP) were incorporated as an insoluble antioxidant into commercially available MTA (CMTA), and the odontoblastic differentiation of human DPSCs was investigated.

Methods. The CMTA was fabricated from MTA and CNP conjugation up to 4 wt%, and the compressive strength, surface morphology after setting and setting time were investigated. Furthermore, the alkaline phosphatase (ALP) assay, Alizarin Red staining (ARS) and quantitative real-time polymerase chain reaction (qPCR) were performed to evaluate odontoblastic differentiation in an indirect co-culture system using inserts with pores. To reveal the underlying mechanism, the ROS levels and ion release were measured. Statistical analysis was performed by one-way analysis of variance with a Tukey post hoc test ($P < 0.05$).

Results. CMTA significantly elevated the odontoblastic differentiation of hDPSCs measured by ALP activity, ARS, and odontoblastic gene expression, whereas the other physico-mechanical properties were relatively maintained. Upregulation of gene expression from CMTA was reversed with hydrogen peroxide. CMTA could reduce the increased intracellular ROS levels of hDPSCs by approximately 70% during differentiation, similar to when an antioxidant was used, without changing the ion release and pH of the media.

* Corresponding authors at: Institute of Tissue Regeneration Engineering (ITREN), Dankook University, Cheonan 31116, Republic of Korea.
** Corresponding author at: Department of Biomaterials Science, College of Dentistry, Dankook University, Cheonan 31116, Republic of Korea.

E-mail addresses: iris979@hanmail.net (S.-K. Jun), 72160525@dankook.ac.kr (J.-Y. Yoon), cmbbsr@gmail.com (C. Mahapatra), kimhw@dku.edu (H.-W. Kim), duciuous@gmail.com (J.-H. Lee), haelee@dankook.ac.kr (H.-H. Lee).

<https://doi.org/10.1016/j.dental.2019.05.024>

0109-5641/© 2019 The Academy of Dental Materials. Published by Elsevier Inc. This is an open access article under the CC BY-NC-ND license (<http://creativecommons.org/licenses/by-nc-nd/4.0/>).

Significance. CMTA could be useful dental materials for regenerating dentin-pulp complexes by instructing intracellular ROS during differentiation to achieve beneficial biological functions. This study suggests a new direction of dental nanomaterials in treating pulp-dentin complexes.

© 2019 The Academy of Dental Materials. Published by Elsevier Inc.

This is an open access article under the CC BY-NC-ND license (<http://creativecommons.org/licenses/by-nc-nd/4.0/>).

1. Introduction

Regeneration of the dentin-pulp complex is the most important biological phenomenon for maintaining tooth viability after dental decay is treated [1–4]. Exciting progress is being made in this field, which utilizes mesenchymal stem cells (MSCs) from dental pulp tissues and promotes natural repair of dental tissue through biomolecules or biomaterials [5–8]. Recent clinical studies have revealed the potential of implanted biomaterials (i.e., mineral trioxide aggregate (MTA) and calcium hydroxide) for accelerating dentin-pulp complex regeneration [9,10]. However, currently available biomaterials are still suboptimal for supporting dentin-pulp complex regeneration due to insufficient odontoblastic differentiation potential, which drives MSCs in the pulp tissue to mature functional cells (odontoblasts) during regeneration.

Acceleration of odontoblastic/osteoblastic differentiation in MSCs would be achieved from a new class of bio-instructive material that regulates intracellular reactive oxygen species (ROS) production [11,12]. During differentiation, intracellular ROS levels increase and mitigate differentiation efficiency. Antioxidant biomolecules such as vitamin C and N-acetylcysteine (NAC) were supplemented in a biomaterial-stem cell co-culture system, including MTA-human dental pulp stem cells (hDPSCs), to detoxify the microenvironment via ROS downregulation and successfully accelerate differentiation [13,14]. However, there is a limitation of applying the above antioxidant biomolecules in the MTA system in clinical settings due to the burst release and non-continuous efficacy of antioxidants in dynamic microenvironments [15,16].

Thus, antioxidants with continuous efficacy and high biocompatibility have been a promising alternative additive [17,18]. Recently, inorganic metal (gold, silver, platinum, selenium) or metal oxide (ceria) nanoparticles exhibited intrinsic redox activity and have been utilized as insoluble biocompatible antioxidants in various medical devices for hard- or neuro-tissue regeneration [19–27]. Here, ceria nanoparticles (CNP) was chosen as a model for incorporating MTA to achieve sustained antioxidant ability during odontoblastic differentiation of hDPSCs.

During differentiation into odontoblasts from hDPSCs, intracellular ROS are upregulated, alleviating the differentiation capacity. Thus, myriad antioxidants (i.e. vitamin C and NAC) have been added to the hDPSC differentiation condition to detoxify the microenvironment via ROS downregulation and accelerate odontoblastic differentiation [13,14]. However, application of the above antioxidants in the MTA system is limited due to the burst release of antioxidants and discon-

tinuous antioxidant effects in dynamic microenvironments. Thus, insoluble antioxidants, capable of revealing consistent antioxidant capacity, with high biocompatibility have been suggested as a promising alternative additive.

Ceria is CeO_2 (cerium oxide) and belongs to the rare-earth elements. Recently, inorganic CNP has been utilized as an insoluble biocompatible antioxidant in a myriad of medical devices for hard- or neuro-tissue regeneration [19–21]. Thus, CNP was mixed in MTA to achieve antioxidant ability during odontoblastic differentiation. After characterization of the physico-mechanical properties of compressive strength and surface morphology after setting time, odontoblastic differentiation was investigated in an indirect co-culture system using inserts with pores. The null hypothesis of this investigation is that there is no difference in odontoblastic differentiation between CNP-incorporated MTA and as-received MTA.

2. Materials and methods

2.1. Synthesis of CNP-incorporated MTA

MTA, consisting of MTA powder, and distilled water (DW) were obtained (Ortho MTA, BioMTA, South Korea; lot number OM1610D15). Ortho MTA consists of tricalcium silicate ($3\text{CaO}\cdot\text{SiO}_2$) 76.3%, dicalcium silicate ($2\text{CaO}\cdot\text{SiO}_2$) 11.8%, tricalcium aluminate ($3\text{CaO}\cdot\text{Al}_2\text{O}_3$) 8.0%, tetracalcium aluminoferrite ($4\text{CaO}\cdot\text{Al}_2\text{O}_3\cdot\text{Fe}_2\text{O}_3$) 0.8% and free calcium oxide (Free CaO) 0.7% as weight % and revealed similar clinical outcomes compared to ProRoot MTA [28]. A CNP sol-gel was fabricated and characterized by transmission electron microscopy for morphology and TMB (3,3',5,5'-tetramethyl-benzidine) assay with hydrogen peroxide for catalytic effect (antioxidant effect) according to previous protocols [20,29]. CNP were incorporated as an additive in quantities of 0.5%, 1%, 2%, and 4% by weight relative to the amount of MTA powder. MTA powder only (0% CNP) was used as control. After mixing the materials mechanically using a rolling ball mill for 24 h, DW was added to the powder at a ratio of 1:1 liquid (mL) to powder (g). After the setting time, disc ($h = 2$ mm and $d = 6$ mm) specimens were made. All tools, including the spatula and mould, were sterilized with ethylene oxide gas before biological testing [30].

2.2. Physico-mechanical properties

The CNP-incorporated MTA disc specimens ($\varnothing = 10$ mm, $d = 2$ mm) were set and polished using SiC paper (up to 1200 grit), and surface morphology was characterized by scanning electron microscopy (SEM, Sigma 500, ZEISS, Jena, Germany). Compressive strength was measured according to ISO 6876

[31]. Briefly, after the powder was mixed with DW, the resulting MTA was inserted into metal moulds (thickness = 6 mm and diameter = 4 mm) and allowed to set at 37 °C (n = 10). After 1 day, compressive strength was measured using an Instron 5966 machine (MA, USA) with a 10 kN load cell at a speed of 1.0 mm/min [32]. The compressive strength (MPa) was determined by dividing the maximum load force before fracture (N) by the area (mm) of the specimen. The setting time was measured according to the standards for root canal sealing materials (ISO 6876, n = 3) [31]. The CNP 0% (MTA) and CNP 4% specimens were chosen as representative materials among experimental groups due to their similar compressive strength regardless of CNP amount conjugated in MTA. Briefly, 30 min after the MTA mixing was started, a Teflon mould ($\Phi = 10$ mm, d = 2 mm) was filled and placed on a Teflon block, and the MTA was maintained at 37 °C and 95% humidity during the measurements. The initial time of the specimens was marked using a Gillmore needle at 30 s intervals. Then, a 1/4-pound flat-end indenter needle was applied vertically to the horizontal surface of the specimens for 5 s. The setting time was independently recorded (n = 3).

2.3. Cytocompatibility test

Primary hDPSCs from a non-carious third molar were cultured between the third and ten passages and were used in this study throughout the *in vitro* experiments after the experimental protocol was approved by the Institutional Review Board (H-1407/009/004) [33]. A cytotoxicity test was performed based on ISO 10993-5. After the cells were seeded (6×10^4 cells/24-well plate) and incubated at 37 °C in a humidified atmosphere of 5% CO₂ and 95% air, each specimen was placed on an insert with 3 μ m pores and co-cultured for 1 day. The disc (thickness = 2 mm and diameter = 6 mm) specimens were made with tools sterilized with ethylene oxide gas using a Person EO50 system (Person Medical, Gunpo-si, Gyeonggi-do, Korea) [30]. Alpha-minimum essential medium supplemented with 1% penicillin/streptomycin (Invitrogen, Carlsbad, CA, USA), 10% fetal bovine serum (Gibco, Waltham, MA, USA), 0.1 mM L-ascorbic acid (Sigma), and 2 mM GlutaMAX (Gibco) was used as the maintaining media (MM) for culturing hDPSCs. The culture volume for the cytotoxicity test with specimen on the insert was initially calculated based on ISO 10993-12 at a ratio of 3 cm²/mL (100%). To immerse the specimen on the insert, the culture media in a well were further adjusted to two (50%) and four (25%) times the original calculated media volume. After 24 h of incubation, cell viability was assessed by the MTS assay by measuring the optical density at 450 nm using a spectrophotometer (SpectraMax M2e, Molecular Devices). MM without specimen was used as control for normalization. To confirm the cytotoxicity results, the live and dead

cells were stained with a commercial kit (LIVE/DEAD™ viability/cytotoxicity kit, ThermoFisher Scientific, Waltham, MA, USA) consisting of calcein AM and ethidium homodimer-1, and images of the live (green) and dead (red) cells were scanned by a digital imaging system (Celena[®] S, Logos Biosystems, Anyang-si, Gyeonggi-do, South Korea).

2.4. Alizarin Red staining (ARS) and alkaline phosphatase (ALP)

To assess the *in vitro* odontoblastic differentiation of hDPSCs, cells (600 μ L of 10⁵/mL) cultured for 24 h with maintaining medium until adherence in 24-well plates were further co-cultured with the determined specimen via the insert in odontogenic differentiation medium (OM, 1256 μ L, 25% condition) that included 50 μ g/mL ascorbic acid, 100 nM dexamethasone, and 10 mM β -glycerophosphate, as described previously [8]. OM and MM without specimen co-culture was used as positive and negative control, respectively. Every 2–3 days, the medium was changed. At specific days, the differentiated cells were fixed with 10% paraformaldehyde for 30 min and rinsed with a phosphate-buffered solution before further staining. At 7 and 14 days, biomineralization measured by ALP activity was visualized by staining using a Sigmafast BCIP[®]/NBT tablet (Sigma) according to the manufacturer's recommendation. On day 21, the cells were stained with a 2% ARS solution (pH 4.2) for 30 min [34]. After being stained and washed five times with DW, images were taken by light microscopy (Olympus IX71, Shinjuku, Tokyo, Japan). All analyses were independently performed in triplicate, and the representative images are shown.

2.5. Real-time polymerase chain reaction (PCR) analysis for odontogenic gene expression

After 7 days of odontogenic induction with the specimens from all the groups described above, real-time PCR was performed according to the manufacturers' protocols. As an antioxidant treatment group, NAC (5 mM, Sigma) was supplemented in OM. As a high-ROS-condition model, hydrogen peroxide (0.1 mM) was added to OM with CNP 4%. Briefly, total RNA was extracted using an RNA purification kit (GeneAll, Ribospin TM, Seoul, Korea), and 2 μ g of total RNA was reverse transcribed to cDNA using the AccuPower RT Premix (Bioneer, Daejeon, Korea) and a model 2720 Thermal Cycler (Life Technologies, Foster City, CA, USA). The quantitative PCR (qPCR) experiments were performed using the RealAmp SYBR qPCR master mix (GeneAll) and a real-time PCR system (StepOne-Plus, Applied Biosystems) according to the manufacturers' instructions. The differential expression of three odontogenic genes (dentin matrix acidic phosphoprotein 1 (DMP1), dentin

Table 1 – Sequence of primer for PCR.

No.	Origin	Gene	Forwar primer sequence 5'–3'	Reverse primer sequence 5'–3'
1	Human	β -actin	CATGGATGATGATATCGCCGCG	ACATGATCTGGGTGATCTTCTCG
2	Human	DSPP	AGAAGGACCTGGCCAAAAAT	TCTCCTCGGCTACTGCTGTT
3	Human	DMP-1	CAGGAGCACAGGAAAAGGAG	CTGGTGGTATCTTCCCCCAGGAG
4	Human	OCN	GTGCAGCCTTGTGTCCAAGCAGGA	CCGTAGAAGCGCCGATAGGCC

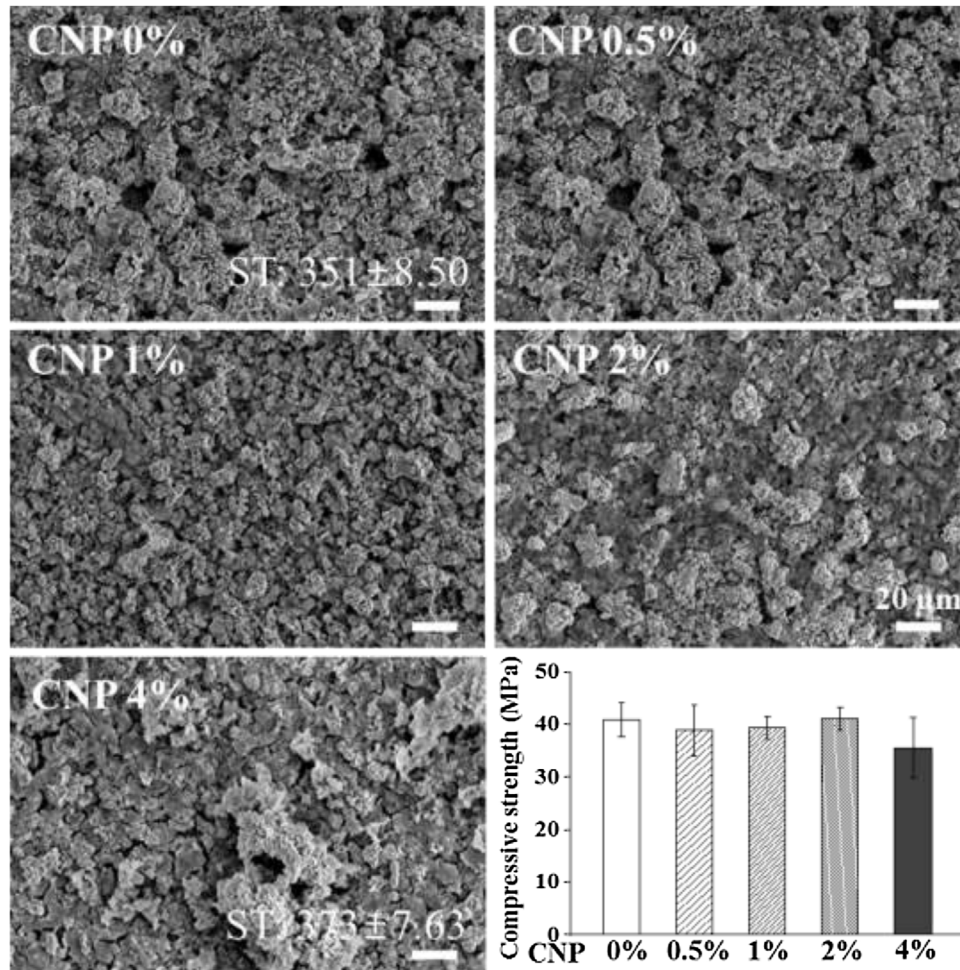


Fig. 1 – SEM images and mechanical properties of ceria nanoparticle (CNP)-incorporated mineral trioxide aggregates (MTA). Different weights of CNP were incorporated into the MTA powder at up to 4%. The surface was rough in all groups after setting and CNP 2% and 4% seemed to have more aggregates than others. The setting time (ST) increased approximately 22 min for CNP 4% compared to that for the MTA control. Compressive strength was maintained regardless of CNP incorporation.

sialophosphoprotein (DSPP) and osteocalcin (OCN) was analysed and normalized to that of β -actin. The primer sequences used are listed in Table 1. After confirming the qPCR efficiency (90–110%) of each gene using ten-fold serial dilutions of cDNA, the positive controls, no-amplification controls and no-template controls were used to confirm the reliability of qPCR without any contamination according to the literature. The relative fold-change in expression was automatically calculated using the $2^{-\Delta\Delta C_t}$ value relative to that of unstimulated hDPSCs (with OM) using StepOne software v2.3. The representative means ($n=4$) were recorded for each sample, and the means with standard deviations (SDs) were calculated ($n=3$) for independent triplicate experiments.

2.6. Released ions and pH change

Representative CNP 0% (MTA) and CNP 4% specimens were chosen for investigating possible factors that affect odontoblastic differentiation. Each specimen was incubated in alpha-minimum essential medium (1 specimen/1256 μ L, 25%

condition). The release of calcium (Ca), silicate (SiO_3), and bismuth (Bi) ions from the extract was measured at a ratio of 3 cm^2/mL with inductively coupled plasma atomic emission spectrometry (ICP-AES) ($n=3$, Optima 4300DV, PerkinElmer, Waltham, MA, USA) according to a previous procedure [35]. The detection limit was 0.1 ppm. After filtering the eluent, 1% nitric acid (15 μ L) was added to 1.5 mL extract media before measurement. The changes in pH during culture were measured with a digital pH meter ($n=3$, Orion 4 Star, Thermo Scientific Pierce, IL, USA) at each time point up to 21 days with media change every 2–3 days. After calibration, the pH of the media was measured as a vehicle control (7.6 ± 0.1) according to the manufacturer's protocol [33]. To confirm reproducibility, all measurements were independently performed in triplicate. The representative means ($n=3$) \pm SDs are shown.

2.7. Inhibited ROS

The generation of intracellular ROS was detected using the CellROX™ Orange reagent (1987206, Invitrogen, Thermo

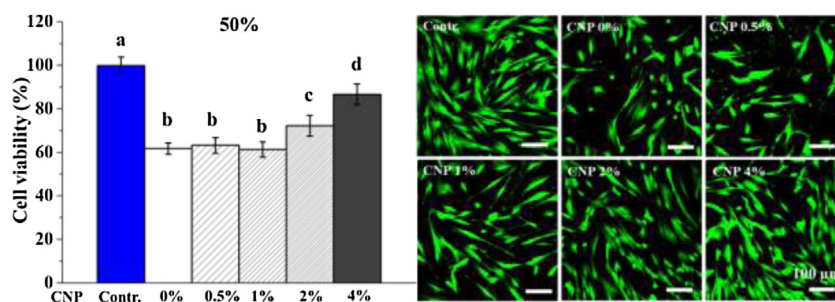


Fig. 2 – Cytocompatibility of CNP-incorporated MTA. Increased CNP incorporation into MTA alleviated the low survivability of human dental pulp stem cells (hDPSCs, $P < 0.05$) caused by a toxic extract (diluted two times (50%) from the ISO standard extract condition) from the original MTA when MTA was co-cultured with hDPSCs for 24 h, as confirmed by the live (green) and dead (red) images. The significant decrease in hDPSC survivability from the as-received MTA was recovered by the CNP-incorporated MTA. The different letters indicate statistically significant differences between their corresponding values ($P < 0.05$). The scale bar is 100 μm . (For interpretation of the references to colour in this figure legend, the reader is referred to the web version of this article.)

Fisher Scientific, USA). Briefly, the cells (600 μL of $10^5/\text{mL}$) were cultured for 24 h with MM until adherence in 24-well plates and were challenged with hydrogen peroxide (0.5 mM) for 30 min under MM or OM along with the CNP 0% or 4% specimen; 5 μM of the CellROX™ Oxidative Stress Reagent working solution was further incubated for 1 h in the dark in a 37 °C incubator. The fluorescence of intracellular ROS was captured by a digital imaging system and quantified by ImageJ (NIH, USA, ver. 1.52a). NAC (5 mM, Sigma) treatment was used for the antioxidant positive group.

2.8. Statistical analysis

The data are expressed as the mean \pm SD of at least three independent experiments. Statistical significance at a value of 0.05 was evaluated via one-way analysis of variance with a Tukey post hoc test using SPSS (Version 21.0; SPSS, Chicago, IL).

3. Results

3.1. Physico-mechanical characterization of commercially available MTA (CMTA)

Along with previous literatures, CNP was successfully sol-gel processed with typical morphology, visualized by TEM, and antioxidant (catalytic) effects (Supplementary Fig. 1). Then, up to 4 wt% sol-gel processed CNP were evenly incorporated into the MTA powder using a rolling machine and mixed with DW at a ratio of 1:1 (powder (g): liquid (mL)) for setting. The surface morphology of the set CMTA was visualized by SEM. A rough surface appeared with a wide range of granule sizes from all groups. CNP 2% and 4% seemed to have higher amounts of ‘aggregates’ on the surface compared to others (Fig. 1). Compressive strength was tested to analyse whether CNP mitigate the mechanical strength of set MTA, revealing no significant decrease in compressive strength up to 4 wt% incorporation. Lastly, the setting time was measured according to ISO 6876, showing a slight increase (approximately 6%)

in setting time from 351 ± 8.5 min (CNP 0%) to 373 ± 7.63 min (CNP 4%, $P < 0.05$).

3.2. Cytocompatibility test

The viability of the hDPSCs was investigated using biomimetic experimental conditions in which CMTA, placed on an insert with a 3 μm pore size to mimic the size of dentinal tubules, was co-cultured with the hDPSCs, and the extract from CMTA could interact with adherent hDPSCs via pores in the insert. At 100% extract culture conditions, the specimen was not fully immersed under the media for 24 h. Thus, 50% extract culture conditions were initially chosen for checking cytocompatibility. The MTA revealed a 40% reduction in cell viability (approximately 60%) compared to that of the control, while CNP 2% and 4% showed an increase in viability up to 70–90% ($P < 0.05$, Fig. 2A). The live and dead images of CNP 0% confirmed the decrease in cell viability, as measured by the above CCK assay, resulting in fewer live (green) and few dead (red) cells than for the control (Fig. 2B). According to the increase in CNP incorporation, more live cells appeared. Under 25% extract culture conditions, cell viability was above 80–90% in all groups under growth condition and differentiated condition (Supplementary Fig. 2), which condition (25% extract culture condition) was further used for odontoblastic differentiation test.

3.3. Odontoblastic differentiation

Odontoblastic differentiation with CMTA was investigated under differentiation media using ALP & ARS staining (Fig. 3) and real-time qPCR assay (Fig. 4). ALP staining after 7 and 14 days of co-culturing revealed an elevation in ALP staining in CMTA, consistent with the increase in CNP incorporation. ARS staining after 21 days indicated a large amount of calcium deposition in the CNP 4% samples. The qPCR results at 7 days indicated an increased expression of odontoblastic markers such as DMP1, DSPP and OCN in CNP 2%, 4% and 0% with NAC (positive control as an antioxidant treatment group) ($P < 0.05$). Odontogenic gene expression was downregulated in cells cul-

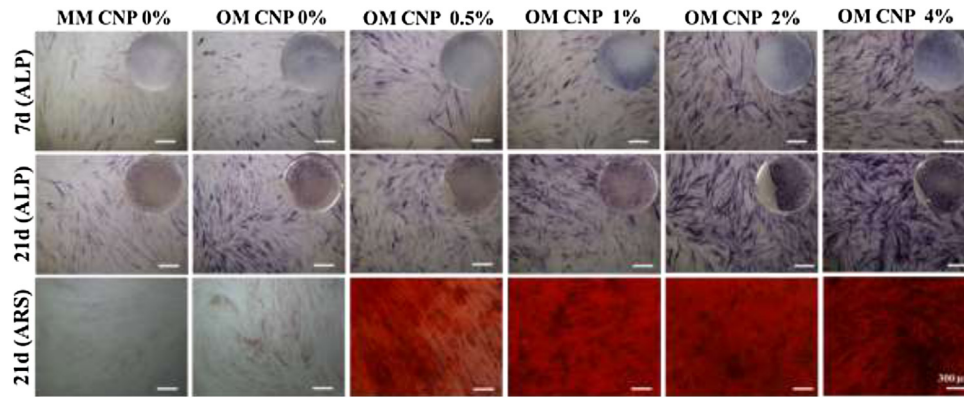


Fig. 3 – Increased odontoblastic differentiation in cells cultured with CNP-MTA. Increase in alkaline phosphatase (ALP) activity (7 and 14 days) and calcium deposition (21 days) evaluated by Alizarin Red S (ARS) staining when MTA was incorporated with CNP. Gradual alleviation of the staining was observed. The scale bar is 300 µm.

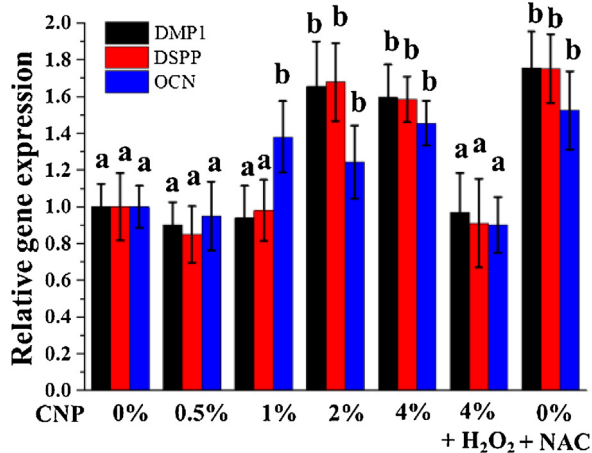


Fig. 4 – Upregulation of odontoblastic differentiation-related gene expression from CNP-MTA. Increased dentin matrix acidic phosphoprotein 1 (DMP1), dentin sialophosphoprotein (DSPP) and osteocalcin (OCN) gene expression levels in cells co-cultured with CNP-MTA (especially CNP 2 and 4%) for 7 days. When hydrogen peroxide was supplemented with CNP 4%, odontogenic gene expression was upregulated. When the antioxidant (NAC) was added with CNP 0%, odontogenic gene expression was enhanced, similar to CNP 4%. The different letters indicate statistically significant differences between their corresponding values ($P < 0.05$).

tured on CNP 4% with hydrogen peroxide compared to that of cells culture on CNP 4% ($P < 0.05$).

3.4. Downregulation of intracellular ROS as a key biological effect

To reveal the underlying mechanism of upregulation of odontoblastic differentiation from CMTA, the amount of ion release, release profiles and pH change were investigated (Fig. 5). Two major therapeutic ions of calcium and silicate were similarly released up to 21 days with similar profile patterns between

CNP 0% and 4%, while another ion of bismuth from bismuth oxide, incorporated in MTA as a radiograph enhancer, was also comparatively leached out. Cerium ions were not detected, and Al ions were detected at less than 1 ppm for up to 21 days in both groups (not shown). The pH change over 21 days was also similar between CNP 0% and CNP 4% (continuously dropping from pH 12 to 9).

Finally, intracellular ROS levels were investigated after 30 min of hydrogen peroxide challenge, followed by 1 h of incubation with CMTA under differentiation media (Fig. 6). The differentiation media induced high intracellular ROS levels (red colour) compared to the growth media ($P < 0.05$), and this high ROS upregulation (approximately 17 a.u.) was significantly mitigated by approximately 30% with CNP 4% and NAC (approximately 5 a.u., $P < 0.05$).

4. Discussion

In the present study, the successful incorporation of therapeutic nano-additive CNP as an antioxidant in MTA was reported for use in pulp-dentin regeneration. Odontoblastic differentiation from hDPSCs is essential for endowing the dentin-pulp complex with regenerative potential when injured and maintaining haemostasis of the pulp-dentin complex. MTA has been successfully applied in clinical settings for regenerating the pulp-dentin complex, but the biological performance of MTA, such as its odontoblastic differentiation ability, is still suboptimal, resulting in failure of pulp-dentin regeneration or repair. One of the promising strategies to enhance the odontoblastic differentiation of MTA is to incorporate functional biomolecules or therapeutic nano-additives. Antioxidants have been highlighted as a promising additive due to their enhanced odontoblastic differentiation ability [36]. During differentiation into odontoblasts from hDPSCs, intracellular ROS are upregulated, alleviating the differentiation capacity. Thus, antioxidants are essential ingredients in odontoblast differentiation media, and further adding antioxidants or preconditioning stem cells with antioxidants synergistically enhances odontoblastic or osteoblastic differentiation [37].

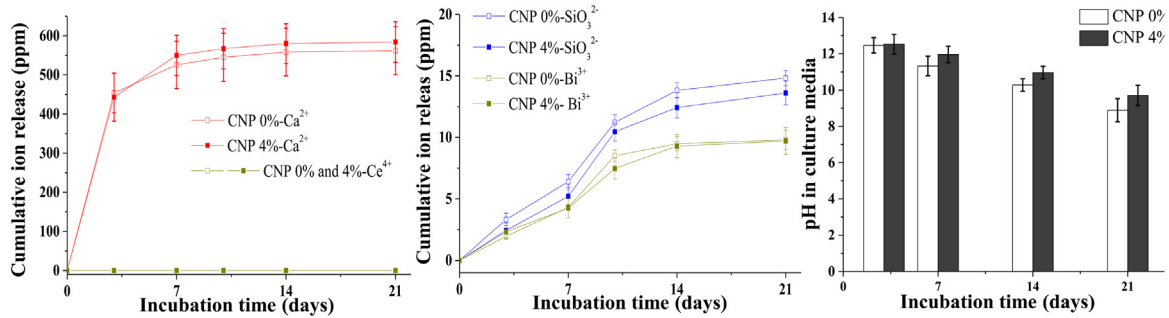


Fig. 5 – Ion release and pH change from CNP-MTA. Comparison of the release of ions (calcium, silicate, and bismuth) in the culture media for up to 21 days between the CNP 0% (MTA) and CNP 4% groups. Cerium ions were not detected in CNP 4%. The pH change over time was similarly detected in the media.

Antioxidants such as vitamin C and NAC were added to the biomaterial-stem cell co-culture system, including the MTA-hDPSC co-culture system, to detoxify the microenvironment via ROS downregulation and accelerate differentiation [13,14]. However, application of the above antioxidant biomolecules in the MTA system in clinical settings is limited due to the burst release of antioxidants in dynamic microenvironments. Thus, insoluble antioxidants with high biocompatibility have been a promising alternative additive. Recently, inorganic CNP has been utilized as an insoluble biocompatible antioxidant

in a myriad of medical devices for hard- or neuro-tissue regeneration [19–21]. Here, CNP in MTA was mixed to achieve antioxidant ability during odontoblastic differentiation.

Adding up to 4 wt% CNP into commercially available MTA powder did not mitigate compressive strength, a key test parameter for resisting biting force, and the outer appearance after setting, which can further influence the ion release profile to affect the biological effects of hDPSCs. Interestingly, a therapeutic role of CMTA was observed in the indirect co-culture system for 1 day using the insert, increasing the via-

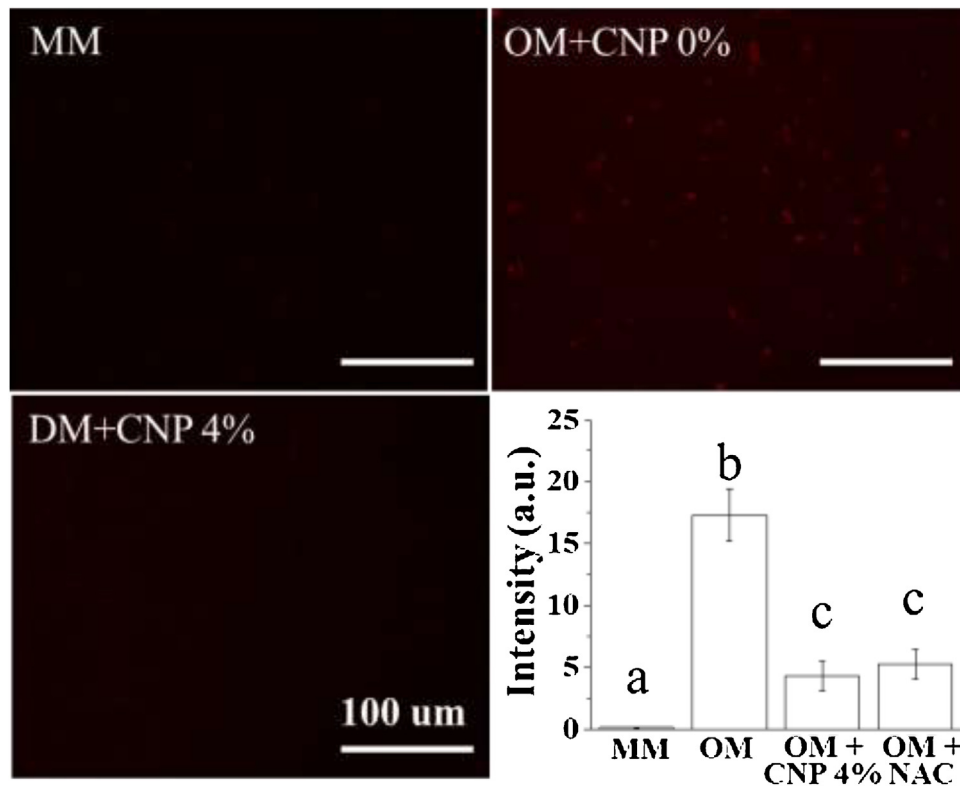


Fig. 6 – Reactive oxygen species (ROS) downregulation of hDPSCs by CNP-MTA. The levels of intracellular ROS (red coloured) in the odontogenic differentiation media (OM) culture system were high compared to that in the maintaining media (MM). The increase in intracellular ROS level under OM significantly decreased with CNP 4%, which might induce efficient odontoblastic differentiation. N-acetyl-L-cysteine (NAC) was used as an antioxidant positive control. The different letters indicate statistically significant differences between their corresponding values ($P < 0.05$). (For interpretation of the references to colour in this figure legend, the reader is referred to the web version of this article.)

bility of the hDPSCs from 60% (CNP 0%; MTA) to 90% (CNP 4%). Upregulation of odontoblastic differentiation was confirmed by ALP and ARS staining, indicating good deposition of phosphate and calcium during odontoblastic differentiation. The upregulation of odontoblastic gene expression markers, such as DMP1, DSPP and OCN, in the CNP 4% group compared to that of the differentiation media control supported the above ALP and ARS staining results. To determine the therapeutic role of CNP 4% in ROS modulation, a non-lethal concentration of hydrogen peroxide was supplemented with CNP 4%, indicating a reduction in upregulated odontogenic gene expression to basal levels. Furthermore, when an antioxidant (NAC) was supplemented with CNP 0%, odontogenic gene expression was enhanced. Taken together, these results suggest that CMTA has a therapeutic role during odontogenic differentiation via ROS modulation (downregulation).

To eliminate the possibility that other factors were involved, the amount of released ions and pH change were investigated in detail. Differently released ions from the biomaterials possibly induced regenerative effects [38–40]. Thus, the amounts of ions and their release profile were compared between CNP 0% and 4%, revealing no significant change in therapeutic (Ca^{2+} and SiO_3^{2-}) and non-therapeutic (Bi^{3+} and Al^{3+}) ion release. Cerium ions were not detected in the CNP 4% group, indicating that CNP, an inorganic additive, was insoluble and that the catalytic effect for ROS modulation (downregulation) was continuous. The basic pH of the culture media was also possibly involved in accelerating odontoblastic differentiation [33]. In this system, the pH changes were similarly for CNP 0% and 4% over 21 days of incubation. Taken together, the results show that the amount of released ions and the pH of the media were not factors affecting odontoblastic differentiation. To confirm the antioxidant role of CNP after incorporating MTA, intracellular ROS were visualized. The small increase in the intracellular ROS level of OM compared to that of GM was not enough to investigate the alleviation of intracellular ROS from CTMA. Thus, we applied sublethal concentrations of hydrogen peroxide (0.5 mM) for 30 min to accelerate the intracellular ROS levels and further co-cultured the cells with CMTA. OM increased the ROS levels up to 17 a.u. compared to that of MM, which was normalized to 0 a.u. When CNP 4% was co-cultured after the medium was changed to OM, the intracellular ROS level decreased by approximately 30% to 5 a.u., similar to the antioxidant effect from NAC. NAC is a well-known antioxidant biomolecule that accelerates odontoblastic differentiation and is used as an antioxidant positive control. Together with the ion release profile and *in vitro* intracellular ROS investigations, these data suggest that the CNP in MTA indirectly provides a therapeutic biological response at a distance via downregulation of intracellular ROS during odontoblastic differentiation of hDPSCs that can improve the state-of-the-art in clinical dentistry for regenerating dentin-pulp complexes.

5. Conclusions

In conclusion, for the first time, this study demonstrated the successful synthesis of incorporating insoluble inorganic CNP into MTA to accelerate odontoblastic differentiation via

ROS downregulation with minimal influence to the physico-mechanical properties of MTA. CNP-incorporated MTA can accelerate odontoblastic differentiation without negatively influencing compressive strength. Thus, CMTA could be useful as dental materials for regenerating the dentin-pulp complex by instructing pathological intracellular ROS for achieving beneficial biological functions.

Author contributions

SK Jun contributed to the conception and design of the study, specimen preparation, and the acquisition (mechanical properties), analysis (mechanical properties), and interpretation of the data; JR-Cha contributed to the conception and design of the study and the acquisition (biopolymer), analysis (biopolymer), and interpretation of the data; HW Kim and JC Knowles contributed to the material, biological and data analysis and critically revised the manuscript; and JH Lee, HR Kim and HH Lee equally contributed to the conception and design of the study, analysis and interpretation of the data, and critical revision of the manuscript. All authors have approved the manuscript and agreed to be accountable for all aspects of this work.

Acknowledgements

This work was supported by the National Research Foundation of Korea (NRF) via a grant funded by the Ministry of Science and ICT (NRF-2019R1C1C1002490, 2018R1C1B5085065, 2018K1A4A3A01064257 (Global Research Development Center Program)) and the Ministry of Education (2019R1A6A1A11034536). This work was also supported by the Innopolis Foundation grant funded by the Korea government(MSIT) (No. 2017-DD-RD-0030-02).

Appendix A. Supplementary data

Supplementary material related to this article can be found, in the online version, at doi:<https://doi.org/10.1016/j.dental.2019.05.024>.

REFERENCES

- [1] Xuan K, Li B, Guo H, Sun W, Kou X, He X, et al. Deciduous autologous tooth stem cells regenerate dental pulp after implantation into injured teeth. *Sci Transl Med* 2018;10, eaaf3227.
- [2] Khayat A, Monteiro N, Smith EE, Pagni S, Zhang W, Khademhosseini A, et al. GelMA-encapsulated hDPSCs and HUVECs for dental pulp regeneration. *J Dent Res* 2017;96:192–9.
- [3] Leyendecker Junior A, Gomes Pinheiro CC, Lazzaretti Fernandes T, Franco Bueno D, et al. The use of human dental pulp stem cells for *in vivo* bone tissue engineering: a systematic review. *J Tissue Eng* 2018;9:2041731417752766.
- [4] Lee J-H, Lee H-H, Kim H-W, Yu J-W, Kim K-N, Kim K-M. Immunomodulatory/anti-inflammatory effect of ZOE-based dental materials. *Dent Mater* 2017;33:e1–12.

- [5] Kaukua N, Shahidi MK, Konstantinidou C, Dyachuk V, Kauka M, Furlan A, et al. Glial origin of mesenchymal stem cells in a tooth model system. *Nature* 2014;513:551.
- [6] Lee JH, El-Fiqi A, Mandakhbayar N, Lee HH, Kim HW. Drug/ion co-delivery multi-functional nanocarrier to regenerate infected tissue defect. *Biomaterials* 2017;142:62–76.
- [7] Chalisserry EP, Nam SY, Park SH, Anil S. Therapeutic potential of dental stem cells. *J Tissue Eng* 2017;8:2041731417702531.
- [8] Lee J-H, Mandakhbayar N, El-Fiqi A, Kim H-W. Intracellular co-delivery of Sr ion and phenamil drug through mesoporous bioglass nanocarriers synergizes BMP signaling and tissue mineralization. *Acta Biomater* 2017;60:93–108.
- [9] Moon H-J, Lee J-H, Kim J-H, Knowles JC, Cho Y-B, Shin D-H, et al. Reformulated mineral trioxide aggregate components and the assessments for use as future dental regenerative cements. *J Tissue Eng* 2018;9:2041731418807396-.
- [10] Cao Y, Song M, Kim E, Shon W, Chugal N, Bogen G, et al. Pulp-dentin regeneration: current state and future prospects. *J Dent Res* 2015;94:1544–51.
- [11] Atashi F, Modarressi A, Pepper MS. The role of reactive oxygen species in mesenchymal stem cell adipogenic and osteogenic differentiation: a review. *Stem Cells Dev* 2015;24:1150–63.
- [12] Tan J, Xu X, Tong Z, Lin J, Yu Q, Lin Y, et al. Decreased osteogenesis of adult mesenchymal stem cells by reactive oxygen species under cyclic stretch: a possible mechanism of age related osteoporosis. *Bone Res* 2015;3:15003.
- [13] Minamikawa H, Yamada M, Deyama Y, Suzuki K, Kaga M, Yawaka Y, et al. Effect of N-acetylcysteine on rat dental pulp cells cultured on mineral trioxide aggregate. *J Endod* 2011;37:637–41.
- [14] Yamada M, Tsukimura N, Ikeda T, Sugita Y, Att W, Kojima N, et al. N-acetyl cysteine as an osteogenesis-enhancing molecule for bone regeneration. *Biomaterials* 2013;34:6147–56.
- [15] Washington KS, Bashur CA. Delivery of antioxidant and anti-inflammatory agents for tissue engineered vascular grafts. *Front Pharmacol* 2017;8:659-.
- [16] Zhu Y, Cankova Z, Iwanaszko M, Lichtor S, Mrksich M, Ameer GA. Potent laminin-inspired antioxidant regenerative dressing accelerates wound healing in diabetes. *Proc Natl Acad Sci* 2018;115:6816–21.
- [17] Kim N-Y, Ahn S-G, Kim S-A. Cinnamaldehyde protects human dental pulp cells against oxidative stress through the Nrf2/HO-1-dependent antioxidant response. *Eur J Pharmacol* 2017;815:73–9.
- [18] Gimeno-Mallench L, Mas-Bargues C, Inglés M, Sanz-Ros J, Dromant M, Borrás C, et al. Antioxidant role of microvesicles, activated by genistein, in stem cells. *Free Radic Biol Med* 2018;120:S83–4.
- [19] Kim J-W, Mahapatra C, Hong J-Y, Kim MS, Leong KW, Kim H-W, et al. Functional recovery of contused spinal cord in rat with the injection of optimal-dosed cerium oxide nanoparticles. *Adv Sci* 2017;4:1700034.
- [20] Mahapatra C, Singh RK, Lee J-H, Jung J, Hyun JK, Kim H-W. Nano-shape varied cerium oxide nanomaterials rescue human dental stem cells from oxidative insult through intracellular or extracellular actions. *Acta Biomater* 2017;50:142–53.
- [21] Kargozar S, Baino F, Hoseini SJ, Hamzehlou S, Darroudi M, Verdi J, et al. Biomedical applications of nanocerium: new roles for an old player. *Nanomedicine* 2018;13:3051–69.
- [22] Valgimigli L, Baschieri A, Amorati R. Antioxidant activity of nanomaterials. *J Mater Chem B* 2018;6:2036–51.
- [23] Dashnyam K, Lee J-H, Mandakhbayar N, Jin G-Z, Lee H-H, Kim H-W. Intra-articular biomaterials-assisted delivery to treat temporomandibular joint disorders. *J Tissue Eng* 2018;9:2041731418776514.
- [24] Lee J-H, Lee MY, Lim Y, Knowles J, Kim H-W. Auditory disorders and future therapies with delivery systems. *J Tissue Eng* 2018;9:2041731418808455.
- [25] Henstock JR, Rotherham M, El Haj AJ. Magnetic ion channel activation of TREK1 in human mesenchymal stem cells using nanoparticles promotes osteogenesis in surrounding cells. *J Tissue Eng* 2018;9:2041731418808695.
- [26] Owens GJ, Singh RK, Foroutan F, Alqaysi M, Han C-M, Mahapatra C, et al. Sol-gel based materials for biomedical applications. *Prog Mater Sci* 2016;77:1–79.
- [27] Seo S-J, Chen M, Wang H, Kang MS, Leong KW, Kim H-W. Extra- and intra-cellular fate of nanocarriers under dynamic interactions with biology. *Nano Today* 2017;14:84–99.
- [28] Kang C-M, Kim S-H, Shin Y, Lee H-S, Lee J-H, Kim G, et al. A randomized controlled trial of ProRoot MTA, OrthoMTA and RetroMTA for pulpotomy in primary molars. *Oral Dis* 2015;21:785–91.
- [29] Singh RK, Patel KD, Mahapatra C, Parthiban SP, Kim T-H, Kim H-W. Combinatory cancer therapeutics with nanocerium-capped mesoporous silica nanocarriers through pH-triggered drug release and redox activity. *ACS Appl Mater Interfaces* 2019;11:288–99.
- [30] Lee J-H, Kwon J-S, Moon S-K, Uhm S-H, Choi B-H, Joo U-H, et al. Titanium-silver alloy miniplates for mandibular fixation: in vitro and in vivo study. *J Oral Maxillofac Surg* 2016;74(1622):e1–12.
- [31] ISO 6876. Root canal sealing materials. Switzerland: International Standardization Organization; 2012.
- [32] Lee J-H, Jo J-K, Kim D-A, Patel KD, Kim H-W, Lee H-H. Nano-graphene oxide incorporated into PMMA resin to prevent microbial adhesion. *Dent Mater* 2018;34:e63–72.
- [33] Jun S-K, Lee J-H, Lee H-H. The biomineralization of a bioactive glass-incorporated light-curable pulp capping material using human dental pulp stem cells. *Biomed Res Int* 2017;2017:9.
- [34] Kim D-A, Lee J-H, Jun S-K, Kim H-W, Eltohamy M, Lee H-H. Sol-gel-derived bioactive glass nanoparticle-incorporated glass ionomer cement with or without chitosan for enhanced mechanical and biomineralization properties. *Dent Mater* 2017;33:805–17.
- [35] Jun SK, Kim H-W, Lee H-H, Lee J-H. Zirconia-incorporated zinc oxide eugenol has improved mechanical properties and cytocompatibility with human dental pulp stem cells. *Dent Mater* 2018;34:132–42.
- [36] Shaban S, El-Husseney MWA, Abushouk AI, Salem AMA, Mamdouh M, Abdel-Daim MM. Effects of antioxidant supplements on the survival and differentiation of stem cells. *Oxid Med Cell Longev* 2017;2017:16.
- [37] Watanabe J, Yamada M, Niibe K, Zhang M, Kondo T, Ishibashi M, et al. Preconditioning of bone marrow-derived mesenchymal stem cells with N-acetyl-L-cysteine enhances bone regeneration via reinforced resistance to oxidative stress. *Biomaterials* 2018;185:25–38.
- [38] Boldbaatar K, Dashnyam K, Knowles JC, Lee H-H, Lee J-H, Kim H-W. Dual-ion delivery for synergistic angiogenesis and bactericidal capacity with silica-based microsphere. *Acta Biomater* 2019;83:322–33.
- [39] Lee J-H, Seo S-J, Kim H-W. Bioactive glass-based nanocomposites for personalized dental tissue regeneration. *Dent Mater J* 2016;35:710–20.
- [40] Perez RA, Seo S-J, Won J-E, Lee E-J, Jang J-H, Knowles JC, et al. Therapeutically relevant aspects in bone repair and regeneration. *Mater Today* 2015;18:573–89.